Islamic Azad University

Journal of
Optoelectronical Nanostructures

Autumn 2021 / Vol. 6, No. 4

Research Paper

Study of the Purcell Factor of a Single Photon Source Based on Quantum Dot Nanostructure for Quantum Computing Applications

Mohammad Reza Mohebbifar[*,1]

[1] Department of Physics, Faculty of Science, Malayer University, Malayer, Iran

Received: 27 Sep. 2021
Revised: 19 Oct. 2021
Accepted: 10 Nov. 2021
Published: 15 Dec. 2021

Use your device to scan and read the article online

Keywords:
Energy eigenvalues, Micro-cavity, Micro-laser, Purcell factor, Quantum efficiency

Abstract

Single photon sources are the basis of quantum computing. An optical system including a quantum dot (QD) within the micro-pillar cavity can be a candidate for high quality single photon source. Here, the vacuum Rabi splitting (VRS) of this optical system for different situations was studied. The coupling constant threshold of this Single photon source to start VRS, was calculated for each of these situations. Then, given that the Purcell factor threshold for using single photon source pulses in linear optics quantum computing is $F_P \geq 40$, Purcell factor behavior of this single photon source including a QD with FWHM of 5μeV, was studied. The results showed that to use the single photon pulses of this system in quantum computation ($F_P \geq 40$), the FWHM of micro-pillar cavity must be less than 100μeV. Also, for cavities with normal FWHM range, if coupling constant is greater than 50μeV, then $F_P \geq 40$ and therefore its single photons can be used for quantum computing.

Citation: Mohammad Reza Mohebbifar. Study of the Purcell factor of a single photon source based on quantum dot nanostructure for quantum computing applications.
Journal of Optoelectronical Nanostructures. 2021; 6 (1): 95- 108.
DOI: 10.30495/JOPN.2022.28408.1227

***Corresponding author:** Mohammad Reza Mohebbifar
Address: Department of Physics, Faculty of Science, Malayer University, Malayer, Iran **Tell:** 081-32241165 **Email:** mmohebifar@gmail.com

1. INTRODUCTION

In recent years, quantum fields have been considered by researchers [1-5]. Cavity Quantum Electrodynamics (CQED) is one of the fields of quantum optics that includes the study of the interaction of quantum light emitters and cavity modes [6]. In 1963, Edwin Jaynes and Fred Cummings proposed a theoretical model that analyzed a quantum description of the interaction of a two-level atomic system with a quantized cavity mode [7] In the same year, Paul introduced this model [8] and therefore this model, which is very popular in atomic physics and quantum optics, was named Jaynes-Cummings-Paul Model (JCPM). In CQED, the Rabi frequency is the measure of the coupling intensity between the field and the atom. The Rabi Frequency is the atomic transition frequency between two energy levels in the presence of electromagnetic field and its value is directly proportional to the size of the applied field and the dipole moment and inversely proportional to the Planck constant [6]. A CQED system, depending on its optical parameters, is usually in two Regimes, Weak Coupling Regime and Strong Coupling Regime. By choosing the structure of quantum system and field intensity, Rabi frequency is set to be less than the decay rate of excited states and photons in the cavity. In this case, the interaction of the quantum system and the electromagnetic field is in the weak coupling regime. One of the properties of this regime is that the emitter and cavity modes can be in resonance with each other, which leads to a sudden increase in the spontaneous emission rate and creates a sharp peak in the spontaneous emission spectrum density. This feature makes this regime suitable for photon generation applications such as Vertical Cavity Surface Emitting Laser (VCSEL) [9], Light Emitting Diode (LED) [10] and entangled photons generation. One of the important platforms in a strong coupling regime is quantum information processing in solid-state devices [11]. In this regime, for large coupling constants, the Anti-Bunching phenomenon occurs. This feature is used in single-photon emitters [12]. The Anti-Bunching phenomenon has given rise to a variety of applications, including quantum cryptography [13], quantum repeaters [14] and quantum computation [15]. Quantum computing is the use of quantum theories such as entanglement and superposition to perform computation. By increasing quality factor of cavity and decreasing the volume of the cavity modes, a strong coupling regime between an atom and an optical cavity can be achieved [16].

Micro-pillar cavities are among the resonators in which, by embedding QD, they can trap isolated photonic modes in small volumes. The light radiation in these micro-cavities is well oriented in the direction of the cylindrical axis. These optical systems have a single peak Gaussian mode, so they have the ability to embed QD nanostructure and coupling with it in both strong and weak modes

[17]. Therefore, a QD within micro-pillar cavity is the suitable candidate for single photon sources. Single photon sources are used in quantum computing and quantum information processing [18-21] and have been observed in various optical systems such as color centers in diamond [22], single molecules [23] and QDs [24]. Among these optical systems, QDs are more compatible with industrial techniques and can be easily embedded into the cavity and increase their spontaneous emission rate based on the Purcell effect [25]. The increase in the spontaneous emission rate in the optical quantum systems is called the Purcell effect. In the 1940s, Edward Mills Purcell discovered that when an atom is coupled to a cavity, under certain conditions the spontaneous emission rate of this atom with a factor called the Purcell factor (F_P) could increase by equation (1) [26].

$$F_P = \frac{3Q\lambda^3}{4\pi^2 V n^3} \tag{1}$$

Where V, Q and n are the mode volume, quality factor and refractive index of the cavity, respectively and λ is the wavelength in this cavity. Based on the Purcell effect, the spontaneous emission rate in different photonic environments such as two and three dimensional photonic bandgap materials and cavities can be controlled [27]. It is also used in photonic systems such as single photon sources for applications in quantum information, quantum cryptography and raising the photon generation efficiency [28]. The Purcell factor of single photon sources is one of the important parameters that is important for quantum computing applications. For example to achieve both efficiency and indistinguishability for gate operations for linear optics quantum computation, $F_P \geq 40$ is required [29]. Figure (1) shows an optical system contains a QD nanostructure in planar distributed Bragg reflector (DBR) cavity that called micro-pillar cavity, which can be used as a single photon source [30].

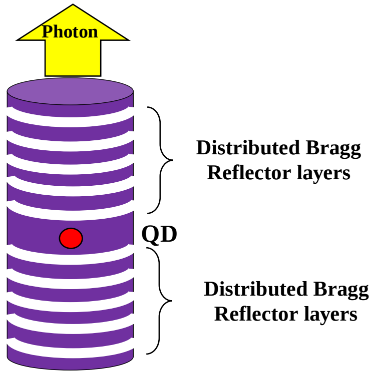

Fig. 1 Scheme of a QD within micro-pillar cavity

In this study, a single photon source including a QD within the micro-pillar cavity was modeled and by analytical solution, first the vacuum Rabi splitting (VRS) and then the Purcell factor behavior for different QDs within different cavities were investigated for use in quantum computing applications.

2. MATERIALS AND METHODS

In order to quantum analysis of this optical system, first the Hamiltonian and then energy eigenvalues for this system were calculated. The QD nanostructure of this system was considered as a two-level atom and the interaction of this two-level atom with a single-mode electromagnetic field was investigated. Since the atom is in resonance or close to one of the cavity modes, only those two levels are important that the frequency of the transition between them is equal to the frequency of the cavity modes. Under such conditions, the excitation of the atom to other levels can be ignored and it can be modeled on the basis of a two-level atomic system. A schematic of this optical system is shown in figure (2).

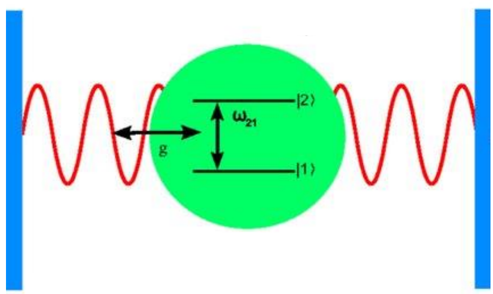

Fig. 2 Scheme of a QD (two-level system) in a cavity [31]

For this two-level atomic system, the Hamiltonian of QD can be expanded based on the ground state $|1>$ and the excited state $|2>$ as follows:

$$H_{QD} = E_1|1><1| + E_2|2><2| \tag{2}$$

Considering the ground state as $|1>=\binom{0}{1}$ and the excited state as $|2>=\binom{1}{0}$, form of the Hamiltonian matrix becomes equation (3).

$$\widehat{H}_{QD} = E\begin{pmatrix}1 & 0\\0 & 1\end{pmatrix} + \frac{1}{2}\hbar\omega_{21}\begin{pmatrix}1 & 0\\0 & -1\end{pmatrix} \tag{3}$$

Where $\hbar$ is the Planck constant divided by 2π and ω_{21} is the transition frequency of two-level atom. The first part of Equation (3) only causes a shift in eigenvalues and has no effect on problem solving, so it can be ignored. $\hat{\sigma}_z = \begin{pmatrix} 1 & 0 \\ 0 & -1 \end{pmatrix}$ is Pauli's matrix and QD Hamiltonian is as follows:

$$\widehat{H}_{QD} = \frac{1}{2}\hbar\omega_{21}\hat{\sigma}_z \tag{4}$$

By embedding QD in the micro-pillar cavity, this QD interacts with electromagnetic field of cavity. The Hamiltonian of interaction (H_I) for such a system can be obtained from the semi-classical approach using the dipole approximation as equation (5) [6].

$$H_I = q\hat{\vec{E}}\hat{\vec{r}} \tag{5}$$

Where q, $\hat{\vec{E}}$ and $\hat{\vec{r}}$ are the electric charge, electric field and position of electron in the nucleus, respectively. $\hat{\vec{r}}$ is an operator and can be expanded on the eigenkets in Dirac notation by equation (6).

$$q\hat{\vec{r}} = P_{22}|2><2| + P_{11}|1><1| + P_{21}|2><1| + P_{12}|1><2|$$
(6)

According to the following equation:

$$P_{\alpha\beta} = e < \alpha|\hat{\vec{r}}|\beta >= \int e\Psi_\alpha^*(\vec{r})\vec{r}\Psi_\beta(\vec{r})\,d^3r$$
(7)

For $\alpha = \beta$ cases, $P_{\alpha\beta} = 0$ and for $\alpha \neq \beta$ cases $P = P_{\alpha\beta} = P_{\beta\alpha}^*$. By defining two operators ξ_1 and ξ_2 as equations (8) and (9), equation (10) is obtained.

$$\xi_1 = |2><1| = \begin{pmatrix} 0 & 1 \\ 0 & 0 \end{pmatrix} \tag{8}$$

$$\xi_2 = |1><2| = \begin{pmatrix} 0 & 0 \\ 1 & 0 \end{pmatrix} \tag{9}$$

$$e\hat{\vec{r}} = P\xi_1 + P^*\xi_2 \tag{10}$$

When operator ξ_1 is applied to the atom in the ground state, the atom is transferred to the excited state and when operator ξ_2 is applied to the atom in the excited state, the atom is transferred to the ground state.

3. RESULTS AND DISCUSSION

By applying the rotating wave approximation, the Hamiltonian of interaction becomes equation (11).

$$H_I = \hbar g\hat{\xi}_1\hat{a} + \hbar g^*\xi_2\hat{a}^\dagger \tag{11}$$

Where g is coupling constant between QD and micro-pillar cavity. Finally, the total Hamiltonian of the system, which is the sum of the Hamiltonian of QD, the Hamiltonian of cavity, and the Hamiltonian of interaction, is as follows:

$$H_T = \frac{\hbar\omega_{21}\hat{\sigma}_z}{2} + \hbar\omega\hat{a}\hat{a}^\dagger + \left(\hbar g\hat{\xi}_1\hat{a} + \hbar g^*\xi_2\hat{a}^\dagger\right) \tag{12}$$

Using total Hamiltonian in the time-independent Schrödinger equation (TISE), energy eigenvalues of a single photon source including a QD within the micro-pillar cavity was obtained as equations (13) and (14).

$$E_1 = \frac{E_c+E_{QD}}{2} - i\frac{\gamma_c+\gamma_{QD}}{4} + \left[g^2 - \left(\frac{\gamma_c-\gamma_{QD}-2i\Delta}{4}\right)^2\right]^{1/2} \quad (13)$$

$$E_2 = \frac{E_c+E_{QD}}{2} - i\frac{\gamma_c+\gamma_{QD}}{4} - \left[g^2 - \left(\frac{\gamma_c-\gamma_{QD}-2i\Delta}{4}\right)^2\right]^{1/2} \quad (14)$$

Where E_c and E_{QD} are the energies of the micro-pillar cavity and QD, γ_c and γ_{QD} are their full width at half maximum (FWHM). It should be noted that the FWHM of micro-pillar cavity and QD represent their decay rates. Also, $\Delta = E_{QD} - E_c$ is the detuning and g is the QD-cavity coupling strength. For resonance state where the cavity frequency is equal to the QD transition frequency, $E_c = E_{QD} = E'$ and consequently Δ becomes zero and equations (13) and (14) becomes as follows:

$$E_1 = E' - i\frac{\gamma_c+\gamma_{QD}}{4} + \left[g^2 - \left(\frac{\gamma_c-\gamma_{QD}}{4}\right)^2\right]^{1/2} \quad (15)$$

$$E_2 = E' - i\frac{\gamma_c+\gamma_{QD}}{4} - \left[g^2 - \left(\frac{\gamma_c-\gamma_{QD}}{4}\right)^2\right]^{1/2} \quad (16)$$

The difference between these two energy eigenvalues indicates Vacuum Rabi splitting (VRS). This parameter shows the difference between the two energy peaks and as a result the energy levels splitting of this optical system (equation (17)).

$$VRS = 2\left[g^2 - \frac{(\gamma_c-\gamma_{QD})^2}{16}\right]^{1/2} \quad (17)$$

If the optical system is designed to be $g^2 - \frac{(\gamma_c-\gamma_{QD})^2}{16} > 0$, the system is in a strong coupling regime, otherwise it is in a weak coupling regime. The higher the VRS parameter of an optical system, the better it is for the anti-bunching phenomenon to occur. This feature is very important in the construction of single photon sources. Also, Purcell factor is another parameter that is very important for single photon sources. Purcell factor used to quantify the performance of quantum information processing systems based on cavity quantum electrodynamics which is expressed by equation (18) [32].

$$F_p = {4g^2}/{\gamma_c\gamma_{QD}} \quad (18)$$

First, calculations were performed using Matlab software (R2018b version) for a single photon source including a QD with a Full width at half maximum (FWHM) of 5μeV embedded in different micro-pillar cavities and the VRS behavior for this optical system was obtained as figure (3).

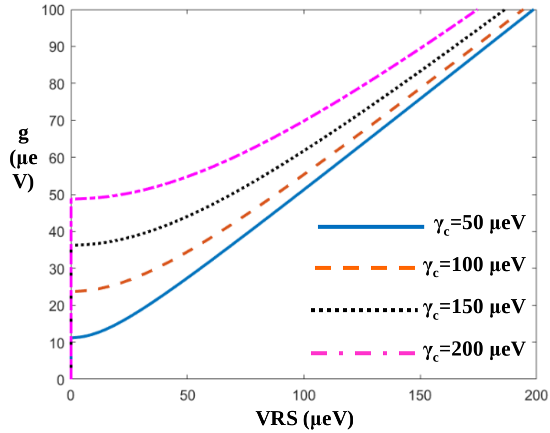

Fig. 3 The VRS behavior for a QD with FWHM of 5μeV in different micro-pillar cavity

The calculations results show that VRS for a single photon source including a QD with FWHM of 5μeV and micro-pillar cavities with FWHMs of 50, 100, 150 and 200μeV [32-34] starts for coupling constants of 11.1, 23.4, 36.4 and 48.7μeV, respectively and with increasing coupling constant, the VRS value also increases. In addition, for micro-pillar cavities with smaller FWHMs (lower decay rates), the rate of VRS changes is higher. Then, different QDs were embedded in a micro-pillar cavity with FWHM of 50μeV, and VRS was calculated for each of them. The results of the calculations are shown in figure (4).

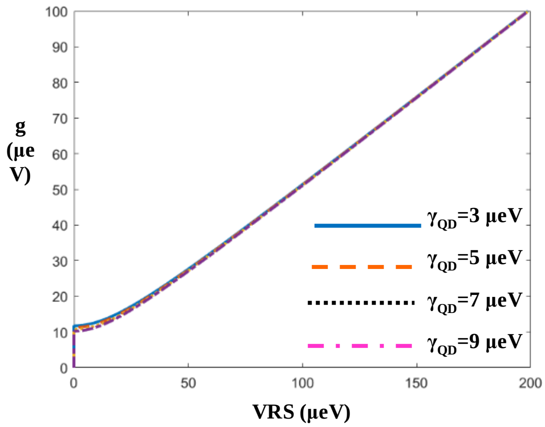

Fig. 4 The VRS behavior for different QD in the micro-pillar cavity with FWHM of 50μeV

The VRS for a single photon source consists of the QD with FWHM of 3, 5, 7, and 9µV embedded in the micro-pillar cavity with FWHM of 50µV starts for coupling constants of 11.7, 10.7, 10.2, and 9.9µeV, respectively. This means that the QD type does not have a significant effect on increasing the VRS of these optical systems.

In the second step, the Purcell factor of this single photon source was investigated. As mentioned in Ref. 21, the Purcell factor threshold for using single photon source pulses in linear optics quantum computing is $F_P \geq 40$. Therefore, the Purcell factor behavior of this single photon source for a QD with FWHM of 5µeV embedded in different micro-pillar cavities with FWHM of 50, 100, 150 and 200µeV are calculated. The results of these calculations are shown in figure (5).

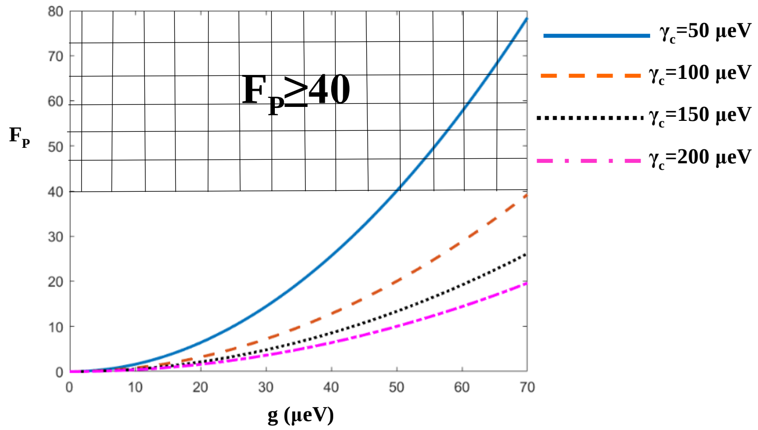

Fig. 5 The Purcell factor behavior for a QD with FWHM of 5µeV in different micro-pillar cavity

The calculation results showed that for this single photon source and at normal coupling constants range, for the micro-pillar cavity with FWHM greater than 100µeV, the Purcell factor is less than 40. Therefore, in order to use the single photon pulses of this optical system in quantum computation, the FWHM of micro-pillar cavity must be less than 100µeV. In addition, the lower the FWHM micro-pillar cavity, the larger rate of increase in Purcell factor.

Then, calculations were performed for a single photon source consisting of a QD with FWHM of 5µeV in micro-pillar cavities with coupling constants of 40, 50, 60 and 70µeV and the behavior of the Purcell factor of these optical systems were investigated. The calculation results are shown in figure (6).

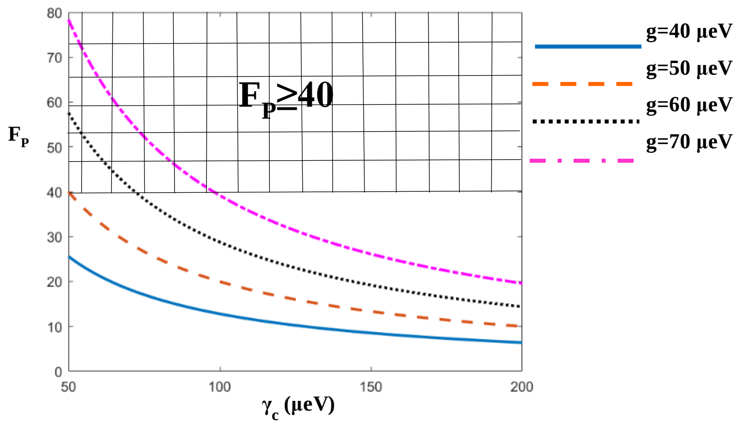

Fig. 6 The Purcell factor behavior for micro-pillar cavities with different coupling constants

The calculation results showed that for micro-pillar cavities with normal FWHM range ($50 \leq \gamma_C \leq 200$), in order to use of these single photon in quantum computing, the threshold of 252 coupling constant must be 50μeV. In addition, to achieve high Purcell factor, micro-pillar cavity with minimum FWHM and maximum g is required. The results showed that to achieve high Purcell factor, micro-pillar cavity with minimum FWHM and maximum g is required. These results can be used in the design of optical quantum systems, single photon sources, and micro-lasers for quantum information, quantum computing, and quantum cryptography.

4. CONCLUSIONS

The calculations results show that VRS for a single photon source including a QD nanostructure with FWHM of 5μeV and micro-pillar cavities with FWHMs of 50, 100, 150 and 200μeV starts for coupling constants of 11.1, 23.4, 36.4 and 48.7μeV, respectively and with increasing coupling constant, the VRS value also increases. While the QD type does not have a significant effect on increasing the VRS of these optical systems. Then, results showed that for this single photon source and at normal coupling constants range, for the micro-pillar cavity with FWHM greater than 100μeV, the Purcell factor is less than 40 and to use the single photon pulses of this optical system in quantum computation, the FWHM of micro-pillar cavity must be less than 100μeV. Also, results showed that for micro-pillar cavities with normal FWHM range ($50 \leq \gamma_C \leq 200$), in order to use of these single photon in quantum computing, the threshold of 252 coupling constant must be 50μeV.

CONFLICT OF INTEREST

The authors declare that there is no conflict of interest regarding the publication of this manuscript.

REFERENCES

[1] M.R. Mohebbifar, *Study of the quantum efficiency of semiconductor quantum dot pulsed micro-laser*, Journal of Optoelectronical Nanostructures, 6 (1) (2021) 59-70. Available: http://jopn.miau.ac.ir/article_4544.html

[2] D. Karimi Moghadam, Gh. Solookinejad, *Implication of Quantum Effects on Non-Linear Propagation of Electron Plasma Solitons*, Journal of Optoelectronical Nanostructures, 5 (3) (2020) 59-70. Available: http://jopn.miau.ac.ir/article_4404.html

[3] R. Yahyazadeh, Z. Hashempour, Numerical Modeling of Electronic and Electrical Characteristics of 0.3 0.7 Al Ga N/Ga N Multiple Quantum Well Solar Cells, Journal of Optoelectronical Nanostructures, 5 (3) (2020) 81-102. Available: http://jopn.miau.ac.ir/article_4406.html

[4] A Horri, S. Z. Mirmoeini, Analysis of Kirk Effect in Nanoscale Quantum Well Heterojunction Bipolar Transistor Laser, Journal of Optoelectronical Nanostructures, 5 (2) (2020) 25-38.

Available: http://jopn.miau.ac.ir/article_4216.html

[5] Abbas Ghadimi; Mohamad Ahmadzadeh, *Effect of variation of specifications of quantum well and contact length on performance of InP-based Vertical Cavity Surface Emitting Laser (VCSEL)*, Journal of Optoelectronical Nanostructures, 5 (1) (2020) 19-34. Available: http://jopn.miau.ac.ir/article_4031.html

[6] W. P. Schleich, *Quantum Optics in Phase Space*, 1st ed., Wiley-VCH, Berlin, (2001).

Available: https://onlinelibrary.wiley.com/doi/book/10.1002/3527602976

[7] E.T. Jaynes, F.W. Cummings, *Comparison of quantum and semiclassical radiation theories with application to the beam maser*, Proceedings of the IEEE, 51(1) (1963) 89-109.

Available: https://ieeexplore.ieee.org/document/1443594

[8] H. Paul, *Induzierte Emission bei starker Einstrahlung*, Ann. Phys., 466(1) (1963) 411-412.

Available: https://onlinelibrary.wiley.com/doi/10.1002/andp.19634660710

[9] V. Bulovic, V. B. Khalfin, G. Gu, and P. E. Burrows , *Weak microcavity effects in organic lightemitting devices*, Phys. Rev. B, 58(1) (1998) 3730–3740.

Available: https://journals.aps.org/prb/abstract/10.1103/PhysRevB.58.3730

[10] R. B. Fletcher et al., *Spectral properties of resonant-cavity, polyfluorene light-emitting diodes*, Appl. Phys. Lett., 77(2) (2000) 1262-1264. Available:

[11] W. P. Schleich and H. Walther Eds., *Elements of Quantum Information*, Wiley-VCH, Weinheim, Germany, (2007). Available: https://aip.scitation.org/doi/abs/10.1063/1.1287402

[12] K. M. Birnbaum et al., *Photon blockade in an optical cavity with one trapped atom*, Nature, 436(3) (2005) 87-90. Available: https://www.nature.com/articles/nature03804

[13] N. Gisin, et al. *Quantum cryptography*, Rev. Mod. Phys., 74(2) (2002) 145–195. Available: https://journals.aps.org/rmp/abstract/10.1103/RevModPhys.74.145

[14] E. Knill et al., *A scheme for efficient quantum computation with linear optics*, Nature, 409(1) (2001) 46-52.

Available: https://www.nature.com/articles/35051009

[15] W. Dür et al., *Quantum repeaters based on entanglement purification*, Phys. Rev. A, 59(4) (1999) 169-181.

Available: https://journals.aps.org/pra/abstract/10.1103/PhysRevA.59.169

[16] S.E. Morin et al., *Strong Atom-Cavity Coupling over Large Volumes and the Observation of subnatural inthracavity atomic linewidths*, Phys. Rev. Lett., 73(1) (1994) 1489–1492.

Available:
https://journals.aps.org/prl/abstract/10.1103/PhysRevLett.73.1489

[17] P. Michler, *Single Semiconductor Quantum Dots*, NanoScience and Technology, Springer, (2009) 267.

Available: https://link.springer.com/book/10.1007/978-3-540-87446-1

[18] D.J. Mowbray and M.S. Skolnick, *New physics and devices based on self-assembled semiconductor quantum dots*, J. Phys. D Appl. Phys. 38(1) (2005) 2059-2076. Available: https://ur.booksc.eu/book/22756298/63caed

[19] G.C. Shan, Z.Q. Yin, W. Huang, and C. H. Shek, *Single photon sources with single semiconductor quantum dots*, Front. Phys., 9 (170) (2014). Available: https://link.springer.com/article/10.1007%2Fs11467-013-0360-6

[20] Yu-Fei Yan, Lan Zhou, Wei Zhong, Yu-Bo Sheng, *Measurement-device-independent quantum key distribution of multiple degrees of freedom of a single photon*, Front. Phys., 16 (1) (2021) 11501. Available: https://link.springer.com/article/10.1007/s11467-020-1005-1

[21] G. Long, F. Deng, C. Wang, K. Wen, W. Wang, X. Li, *Quantum secure direct communication and deterministic secure quantum communication*, Front. Phys., 2 (3) (2007) 251-272.

Available: https://link.springer.com/article/10.1007/s11467-007-0050-3

[22] C. Kurtsiefer et al., *Stable Solid-State Source of Single Photons*, Phys. Rev. Lett., 85(5) (2000) 290.

Available: https://journals.aps.org/prl/abstract/10.1103/PhysRevLett.85.290

[23] B. Lounis and W.E. Moerner, *Single photons on demand from a single molecule at room temperature*, Nature, 407 (2000) 491-493. Available: https://pubmed.ncbi.nlm.nih.gov/11028995/

[24] P. Michler, et al., *Quantum correlation among photons from a single quantum dot at room temperature*, Nature, 406 (2000) 968–970. Available: https://www.nature.com/articles/35023100

[25] J.M. Gerard et al., *Enhanced Spontaneous Emission by Quantum Boxes in a Monolithic Optical Microcavity*, Phys. Rev. Lett., 81 (1998) 1110.

Available:
https://journals.aps.org/prl/abstract/10.1103/PhysRevLett.81.1110

[26] Purcell, E. M., *Proceedings of the American Physical Society: Spontaneous Emission Probabilities at Ratio Frequencies*, Physical Review, 69 (1946) 11–12. Available: https://journals.aps.org/pr/abstract/10.1103/PhysRev.69.674.2

[27] Kress, A. et.al, *Manipulation of the spontaneous emission dynamics of quantum dots in two-dimensional photonic crystals*, Physical Review B, 71 (24) (2005) 241304.

Available:
https://journals.aps.org/prb/abstract/10.1103/PhysRevB.71.241304

[28] M. C. Münnix; A. Lochmann; D. Bimberg; V. A. Haisler, *Modeling Highly Efficient RCLED-Type Quantum-Dot-Based Single Photon Emitters*. IEEE Journal of Quantum Electronics, 45 (9) (2009) 1084–1088. Available: https://ieeexplore.ieee.org/document/5191277

[29] A. Kiraz, M. Atatüre, A. Imamoglu, *Quantum-dot single-photon sources: Prospects for applications in linear optics quantum-information processing*, Physical Review A, 69 (2004) 032305. Available: https://journals.aps.org/pra/abstract/10.1103/PhysRevA.69.032305

[30] Ding, X. et al. *On-demand single photons with high extraction efficiency and near-unity indistinguishability from a resonantly driven quantum dot in a micropillar*, Physical review letters, 116 (2016) 020401. Available: https://journals.aps.org/prl/abstract/10.1103/PhysRevLett.116.020401

[31] L. Teuber, P. Grünwald, W. Vogel, *Nonclassical light from an incoherently pumped quantum dot in a microcavity*, Physical Review A, 92(5) (2015). Available:
https://journals.aps.org/pra/abstract/10.1103/PhysRevA.92.053857

[32] D. Press et.al., *Photon Antibunching from a Single Quantum-Dot-Microcavity System in the Strong Coupling Regime*, Phys. Rev. Lett., 98 (2007) 117402.

Available:
https://journals.aps.org/prl/abstract/10.1103/PhysRevLett.98.117402

[33] J. P. Reithmaier, G. Sek, A. Loffler, C. Hofmann, S. Kuhn, S. Reitzenstein, L. V. Keldysh, V. D. Kulakovskii, T. L. Reinecke, A. Forchel, *Strong coupling in a single quantum dot–semiconductor microcavity system*, Nature, 432 (2004) 197-200.

Available: https://www.nature.com/articles/nature02969?proof=t

[34] P. Munnelly, T. Heindel, M. M. Karow, S. Hofling, M. Kamp, Ch. Schneider, S. Reitzenstein, A Pulsed Nonclassical Light Source Driven by an Integrated Electrically Triggered Quantum Dot Microlaser, IEEE Journal of Selected Topics in Quantum Electronics, 21 (6) (2015) 1900609. Available: https://ieeexplore.ieee.org/document/7073594